ENHANCED KNOWLEDGE IN SCIENCES AND TECHNOLOGY
e-ISSN: 2773-6385

EKST

Vol. 4 No. 1 (2024) 312-320
https://publisher.uthm.edu.my/periodicals/index.php/ekst

Characterization of Au Thin Films With Laser Annealing at Different Energies on P-Type Silicon for Flat Panel Display Application

Nur Syamimi Md Khairi[1], Ahmad Hadi Ali[1]*

[1] *LASERG, Physics and Chemistry Department, Faculty of Applied Sciences and Technology, Universiti Tun Hussein Onn Malaysia, UTHM Kampus Cawangan Pagoh,Hab Pendidikan Tinggi Pagoh, KM 1, Jalan Panchor, 84600 Pagoh, Muar, Johor, MALAYSIA*

*Corresponding Author: ahadi@uthm.edu.my
DOI: https://doi.org/10.30880/ekst.2024.04.01.036

Article Info

Received: 26 December 2023
Accepted: 13 June 2024
Available online: 27 July 2024

Keywords

Au Thin Film, Laser annealing, Flat Panel Display, TFT, AFM, Four-point probe, SEM-EDX, UV-Vis.

Abstract

In TFTs, the metal-semiconductor contact links the semiconductor structure to external influences impacting flat panel display functionality. However, due to the inherent amorphous nature of the materials, achieving lower contact resistance and enhanced conductivity are challenging in thin metal contacts. This research involved depositing Au thin film layer by DC sputtering technique onto p-type silicon subsequently annealed using Nd:YAG pulsed laser at different energy levels. The topology, elemental, electrical and optical properties of treated Au thin film were examined via Atomic Force Microscopic (AFM), Scanning Electron Microscopy-Energy Dispersive X-ray spectroscopy (SEM-EDX), Four Point Probe (4PP), and Ultraviolet-Visible Spectroscopy (UV-VIS), respectively. The results indicate annealed gold (Au) thin films exhibit improved conductivity with increasing laser energy, peaking at 170 mJ, and shows the lowest average resisiticity and sheet resistivity with value of 3.19×10^{-4}(Ω/cm) and 80.81 (Ω/sq). Atomic Force Microscopy (AFM) analysis reveals higher average and RMS surface roughness at 170 mJ with value of 9.17 nm and 11.4 respectively. UV-Vis absorbance measurements consistently indicate low absorbance levels below 20%, attributing it to high reflectivity but increasing with laser energy. Elemental composition analysis using SEM-EDX confirms only Au and Si elements. Hence, Nd: YAG laser treatment significantly enhances the electrical and structural properties of Au thin films, evident in conductivity, surface roughness, absorbance, and elemental composition analyses.

1. Introduction

Flat panel displays, such as LCD and OLED screens, are essential components in modern electronic devices, such portable gadgets like laptops [1], monitor [2], television [3], and smartphones [4]. These displays generate images and videos through pixels and rely on thin film transistors (TFTs) to function as switches for individual pixels [5]. Within each TFT section dedicated to a pixel, components like electrodes, select lines, and data lines are crucial, with the select and data lines specifically responsible for loading data into pixels and charging capacitors [6]. Hence, thin metal films are the preferred materials due to their exceptional electrical conductivity and compatibility with semiconductor materials like silicon found within TFT structures [7].

The selection of material significantly impacts the efficiency of the electrical conductivity throughout the TFTs. Therefore, a low data-line resistivity or high conductivity TFTs is required for high resolutions and large display sizes. A specific type of electrical contact such as gold (Au) thin film layer contact suitable to be employed to enable efficient electrical conductivity. Au can establish a low resistance electrical connection to the external circuitry by deposited on substrate materials such as glass or Silicon to facilitate the conduction of electrical current through the flat panel display.

The deposition technique for this thin layer typically involves sputtering processes, which are favoured for their inherent advantages. Sputtering processes offer excellent thickness uniformity compared to evaporation. Moreover, sputtering enables higher deposition rates, ensuring efficient film growth. Subsequently, the properties of deposited films were enhanced by additional post-treatments such as Nd:YAG pulsed laser treatment. The laser energy emitted during the treatment is absorbed by the material, inducing structural rearrangement [8]. This process crucial for recrystallization of the initially amorphous thin film into the development of crystalline or polycrystalline structure [9].

Overall, the aim of this study is to investigate the impact of Nd:YAG pulsed laser treatments at different energy levels on the properties of gold (Au) thin films, including aspect such as topology, elemental composition, electrical and optical properties.

2. Materials and Methods

Initially, Si substrates were cut into 1cm × 1 cm size. Then, the substrates were cleaned by submerged it into acetone solution and heating it at 60°C for 15 minutes using ultrasonic cleaner to eliminate the contamination on sample surface. This step was repeated by using isopropyl alcohol. Next, the substrates cleaned with deionized solution. After cleaning, the samples were inserted inside plasma cleaner and subjected to the Nitrogen gaseous for 15 minutes to remove impurities including water molecules.

Au was deposited intermittently on Si substrate by using DC sputtering system model Q150R S for 10 minutes two times. The base pressure during the sputtering process was ~1×10^{-2} to 1×10^{3} mbar with rotation of sample holder of ~50 rpm. A configuration of deposited thin films consisting of Au metal contacts on Si substrates is shown in **Fig. 1**.

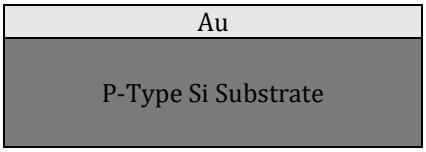

Fig. 1 *The cross-sectional of Au layer deposited on Si substrate.*

Before samples were annealed, the thickness of each deposited Au thin layer was measured by using ellipsometer which is 39.5 nm. The samples then treated with Nd:YAG pulsed laser with wavelength of 1640 nm and the laser was set at 90 mJ, 110 mJ, 130 mJ, 150 mJ, 170 mJ and 190 mJ with 1 cm^2 of the laser spot size with radius of 5 mm. This process was aided by a converging lens with focal length of 8 cm from its axis. Three shots of Nd:YAG pulsed laser were bombard on the samples. **Fig. 2** illustrates the setup for the Nd:YAG laser treatment.

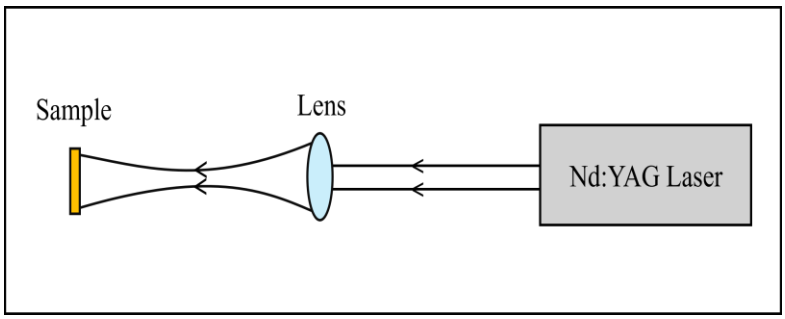

Fig. 2 *Illustration of Nd:YAG laser treatment setup.*

The characterization process begins by examining the surface topological properties of the Au thin film using AFM. This involved assessing film roughness and grain size in a 1 μm × 1 μm area, employing non-contact mode with a force ranging between 10 to 100 nm. AFM images produced, then, were analysed through Nanoscape software. Subsequently, electrical properties were explored through four-point probe analysis, evaluating sample contact quality via an IV curve. Using metallic probes, current injection and voltage

Enhanced Knowledge in Sciences and Technology Vol. 4 No. 1 (2024) p. 312-320

measurement were conducted, and data analysis revealed essential properties such as resistance and resistivity, critical for conductivity measurement. Next, SEM-EDX was used for individual particle spectra analysis, utilizing an electron beam for scanning, peak identification, and intensity quantification through a computer program. Intensity values were then converted into percentage weights to determine elemental composition. Finally, UV-vis spectroscopy was utilized to examine optical properties, focusing on absorption between 300 nm to 600 nm. The analysis yields information about absorption characteristics like peak absorption and intensity at specific wavelengths.

3. Results and Discussion

3.1 Topographical properties

Fig. 2 presents the topography, in 3D, AFM images for thin films of Au deposited on silicon of a 5 nm × 5nm area scan size for both the as deposited and post-treatment samples. It is apparent that variations in laser annealing energy have been shown to alter the size and distribution of the grains due to the absorption of laser heat. The RMS roughness of the treated samples shows a progressive increase from the as-deposited state to the maximum laser energy setting of 190 mJ as the applied laser energy increases. Comparing the post-treatment sample to the as-deposited sample, the sample treated with 190 mJ laser energy had a smoother surface. The surface area with uniform distribution of grains is referred to as this smoothness.

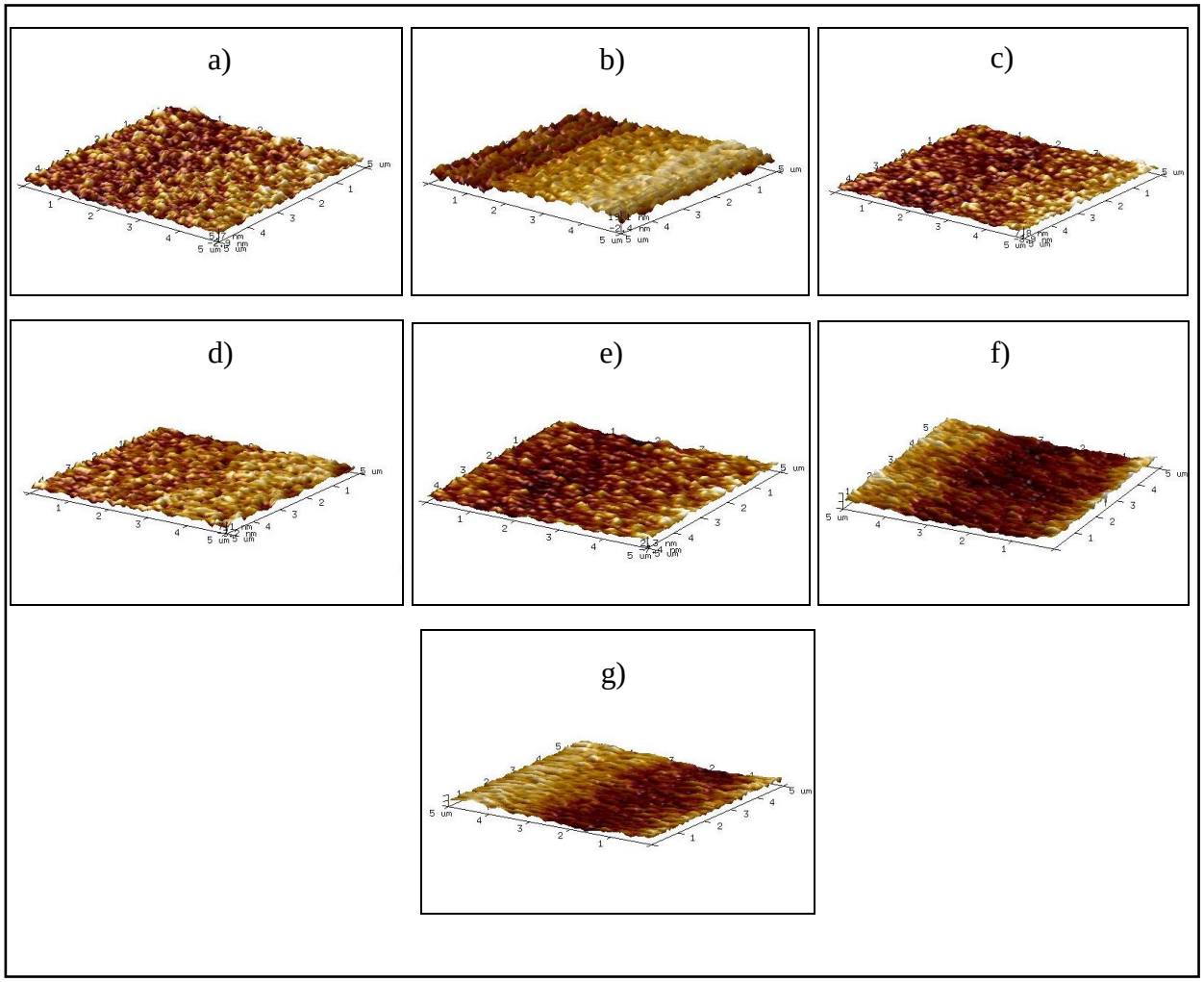

Fig. 2 *AFM 3D images of Au thin films laser annealed in room temperature at (a) As-deposited, (b) 90 mJ, (c) 110 mJ, (d) 130 mJ, (e) 150 mJ, (f) 170 mJ, and (g) 190 mJ.*

The graph in **Fig. 3** shown the differences of RMS and average roughness according to the distinct laser energies. Despite the smoothness and uniform surface of thin film, there are the irregularities of this surface

morphology which represented by both Ra and Rq. There is an increase in Rq and Ra corresponds to an increase in laser energy in which the highest Rq and Ra shown when sample treated at 170 mJ with . This could be explained by considering the thermal annealing induced coalescence of small grains by grain boundary diffusion which caused major grain growth [10]. The grain growth mechanism includes the transfer of atoms at grain boundaries from one grain to another and the final grain depends upon the specific annealing conditions. However, there are minor fluctuations observed, involving certain points where a decrease in roughness occurs such at 90 mJ, 150 mJ and 190 mJ with Rq and Ra value of 1.35 nm and 1.07 nm, 6.19 nm and 4.61 nm, and, 7.60 nm and 5.93 nm, respectively. Similarly, the grain size exhibits a similar pattern to the RMS roughness [11]. The grain growth mechanism includes the transfer of atoms at grain boundaries from one grain to another and the final grain depends upon the specific annealing conditions.

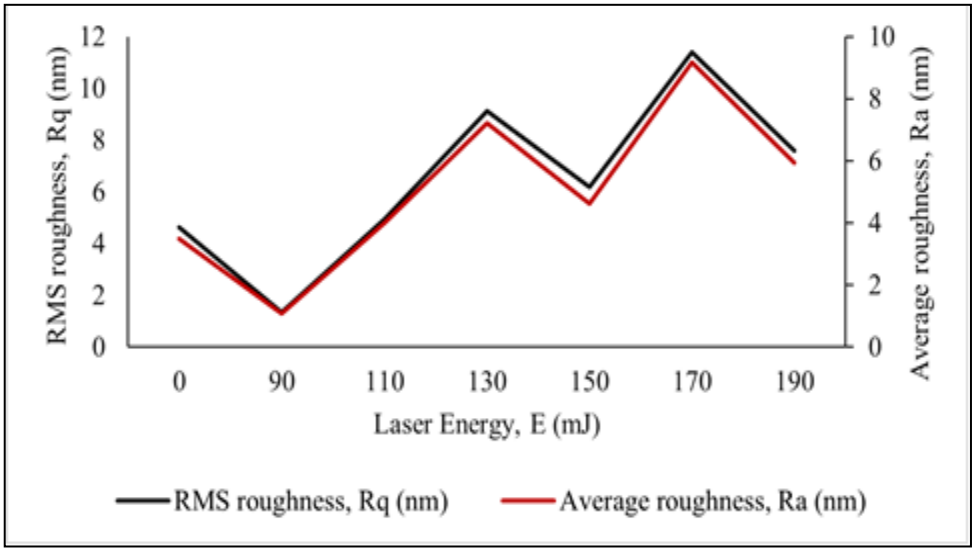

Fig. 3 *Graph of RMS and average roughness of Au thin films against laser energy.*

3.2 Electrical properties

Fig. 4 shows the average and sheet resistivity at different laser energy. All samples exhibited varying values of resistivities despite having the same thickness and conditions. Both average and sheet resistivity show a similar decreasing trend. The observed trend in average resistivity revealed that the sample annealed at 90 mJ displayed the highest resistivity with value 3.58×10^{-4} (Ω/cm) compared to as-deposited sample, 3.50×10^{-4}(Ω/cm) likewise for sheet resistivity with highest value is 90.51 (Ω/sq) as compared to as-deposited sample, 88.54 (Ω/sq). This heightened resistivity observed post-annealing due to structural modifications induced by the annealing process [12]. However, as laser energy increases the average and sheet resistivity become lower especially at 130 mJ and 170 mJ, with value of resistivity, 3.22×10^{-4}(Ω/cm), 81.45 (Ω/sq) and 3.19×10^{-4}(Ω/cm), 80.81 (Ω/sq), respectively. This attributed to the annealing process inducing grain growth in the thin film enhanced the surface structured as well as reducing the resistivity [13]. This finding aligns with the research indicating a strong dependence of an Au thin film's resistivity on its morphology, allowing for real-time monitoring of structural changes within the film [14].

Enhanced Knowledge in Sciences and Technology Vol. 4 No. 1 (2024) p. 312-320

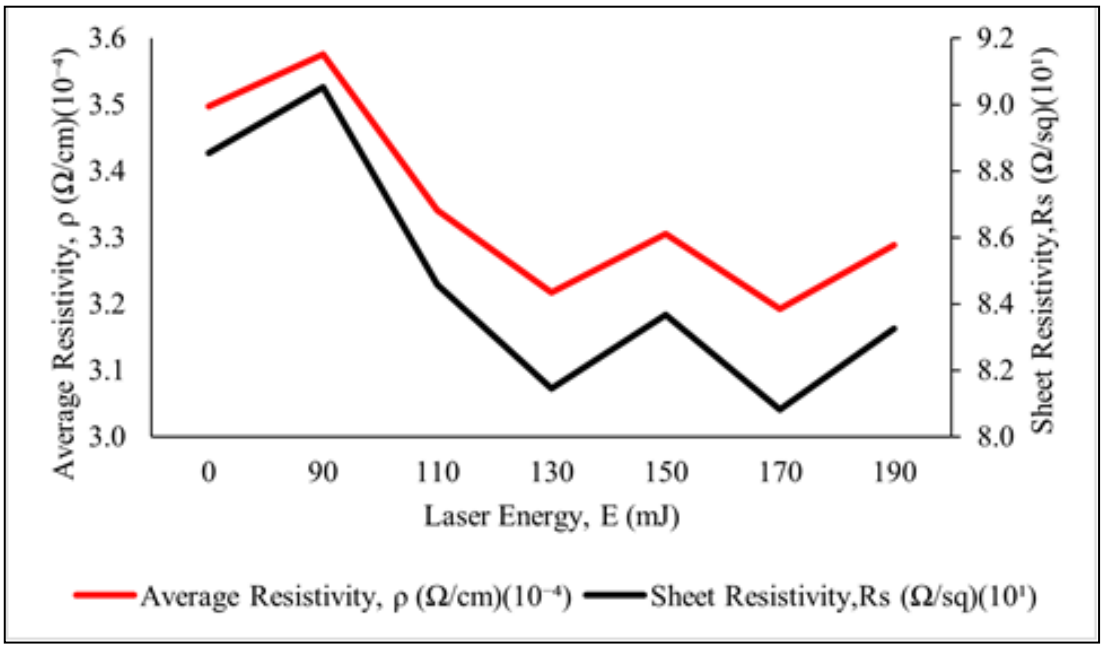

Fig. 4 *The resistivity and sheet resistance observed in Au thin films deposited on silicon in relation to the laser annealing energy.*

Fig. 5 shows the conductivity of each sample at different laser energies. The observed trend contrasts with the resistivity graph, reflecting the inherent nature of the conductivity equation, which is inversely proportional to resistivity. The highest conductivity occurs at 170 mJ with value of $3.04\times10^{3}(\Omega/sq)$, signifying superior ability to oppose current flow. However, at 90 mJ, 150 mJ, and 190 mJ, conductivity slightly decreases, likely influenced by substrate effects [15].

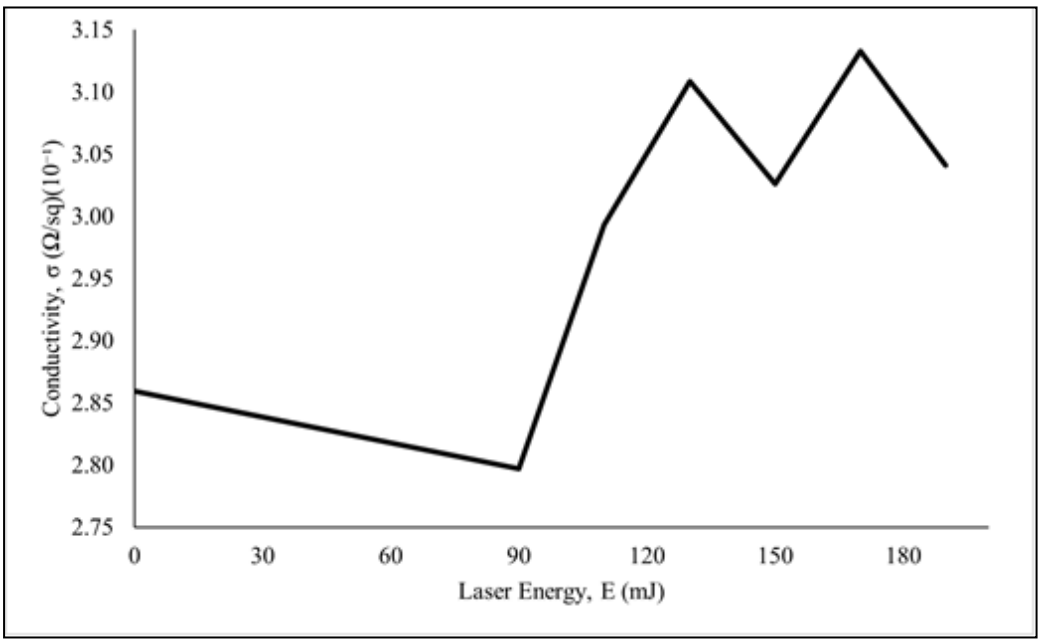

Fig. 5 *The conductivity, σ against laser energy, E for Au thin films.*

3.3 Elemental Composition

SEM-EDX analysis determined the elemental composition of Au thin films by obtaining spectra of individual particles after scanning an electron beam onto the surfaces of the samples. Different peaks were identified, and computer software quantified peak intensities. Analysis performed on samples treated with various laser energies of 90 mJ, 130 mJ, and 170 mJ, revealing no foreign element detected other than Au and Si, as illustrated in Fig. 6. This is corroborated by the scanned images of the thin film surfaces, demonstrating minimal contamination or anomalous shapes, as evident in the grey images.

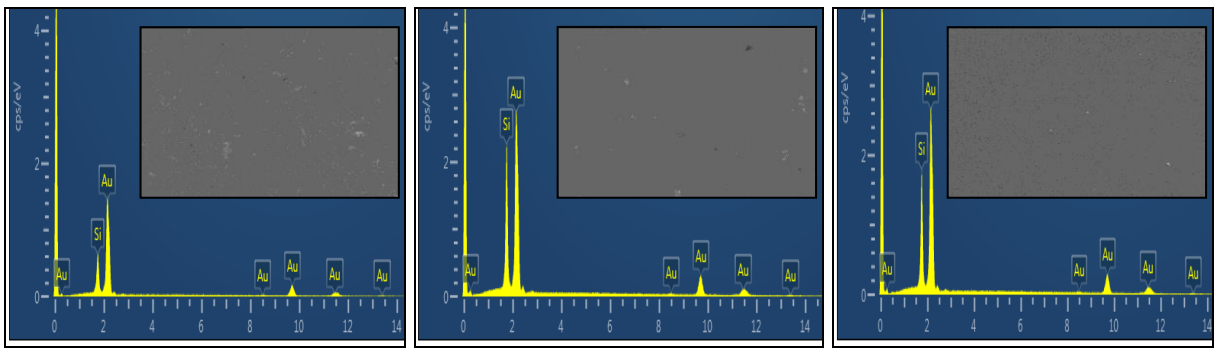

(a)90 mJ (b) 130 mJ (c) 170 mJ

Fig. 6 *The EDX spectrum of Au thin film annealed at (a) 90 mJ, (b) 130 mJ and (c) 170 mJ.*

Table 3 displays converted peak intensities as percentage weights, revealing that higher laser energy correlates with increased weight percentage of Au element, surpassing Si. Although atomic percentage of Au rises with laser energy with value of 42.50%, 46.91% and 57.63%, it remains smaller than Si with atomic percentage of 57.50%, 53.09% and 56.63%, respectively. The short deposition time of 20 minutes, which results in a film not as thick as the Si substrate, leading to a lower atomic percentage of Au compared to Si in the final film. Therefore, the overall percentage is determined by the ratio of the number of Au atoms to the total number of atoms in the film, and with less Au deposited, it naturally makes up a smaller fraction.

Table 3 *The composition element presented for each sample*

(a) 90 mJ		
Element	Weight %	Atomic %
Au	83.83	42.50
Si	16.17	57.50
	100.00	100.00
(b) 130 mJ		
Element	Weight %	Atomic %
Au	86.10	46.91
Si	13.90	53.09
Total	100.00	100.00
(c) 170 mJ		
Element	Weight %	Atomic %
Au	90.51	57.63
Si	9.49	42.37
Total	100.00	100.00

Enhanced Knowledge in Sciences and Technology Vol. 4 No. 1 (2024) p. 312-320

3.4 Optical properties

Fig. 7 revealed the absorbance of Au thin films against wavelength at various laser energies using UV-Vis spectroscopy. Results show consistently lower absorption levels across the UV to visible range (360 nm to 600 nm), with higher laser energy leading to increased absorption. [16] This rise likely occurs due to reduced reflectance and enhanced surface roughness post-annealing. This can be supported by a study which shown annealing process has been shown to improve the granular nanostructure of thin films, leading to an increase in the absorption coefficient [17]. Nonetheless, even after treatment, all analyzed metal films exhibit consistently low absorbance, remaining below 20%. This suggests the films retain high reflectivity, potentially due to the inherent opaqueness of Au thin films [18, 19, 20].

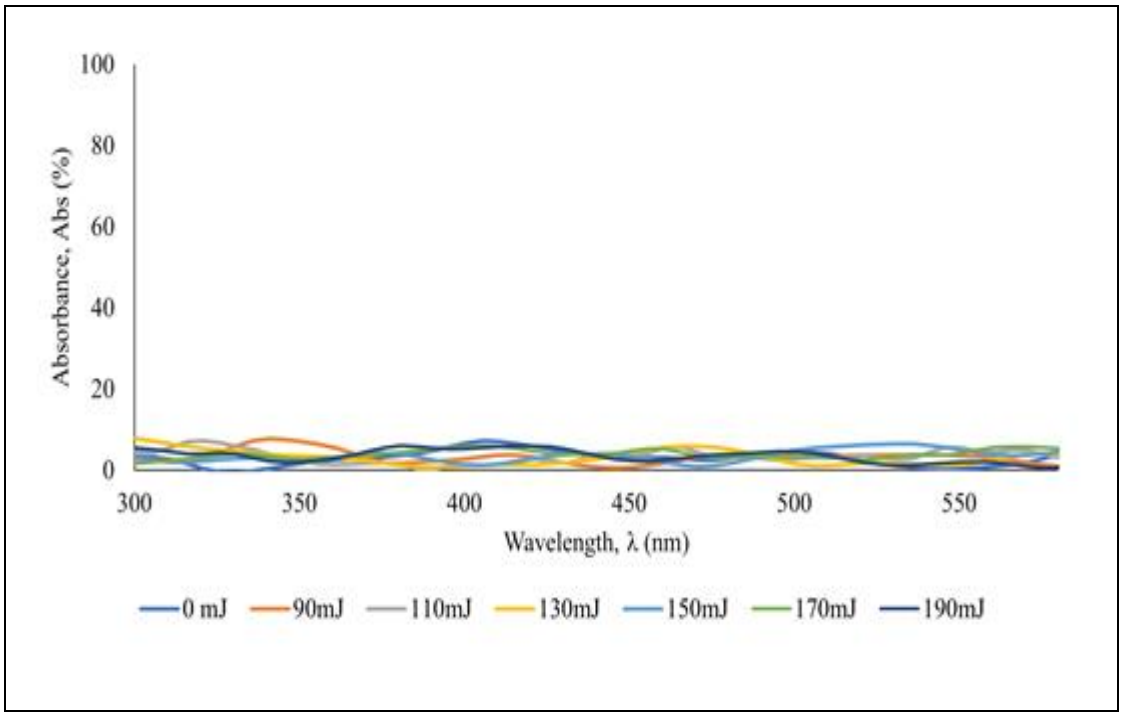

Fig. 7 *The absorption spectra of Au thin films from UV to visible range of wavelengths*

4. Conclusion

This research explored the effects of Nd:YAG laser radiation at different energy levels on gold (Au) thin films deposited via DC sputtering onto silicon (Si) substrates. The findings revealed the AFM analysis shows the highest average and RMS roughness obtained when sample is treated and 170 mJ with value 9.17 nm and 11.4 nm, respectively. Similarly, the sample treated at 170 mJ exhibited the lowest average and sheet resistivity value, 3.29×10^{-4}(Ω/cm) and 83.26 (Ω/sq), respectively. Likewise, the absorption percentage, which obtained using UV-Vis, also increases as energy laser increase although its exhibit very low value of absorption, below 20%. Lastly, SEM-EDX results shows the element consists only Au and Si. To sum up, the investigation revealed that the optimal laser energy to improve the conductivity of Au thin film for flat panel display application is 170 mJ.

Acknowledgement

The author(s) appreciate the Government of Malaysia and Universiti Tun Hussein Onn Malaysia for funding this research project through the UTHM TIER1 Grant (Q417).

Conflict of Interest

Authors declare that there is no conflict of interests regarding the publication of the paper.

Author Contribution

The authors confirm contribution to the paper as follows: ***study conception and design, data collection, methodology, analysis and interpretation of results:*** *Nur Syamimi Md Khairi and Ahmad Hadi Ali. All authors reviewed the results and approved the final version of the manuscript.*

References

[1] A. Khazanchi, A. Kanwar, L. Saluja, A. Damara, & V. Damara. (2012). OLED: A New Display Technology. In International Journal Of Engineering And Computer Science, Volume 1, Issue 2, 75-84.
[2] G. Seong, Y. Lee, & Y. Kwak. (2021). Image quality comparison between LCD and OLED display. IS and T International Symposium on Electronic Imaging Science and Technology, 2021(16). https://doi.org/10.2352/ISSN.2470-1173.2021.16.COLOR-326
[3] Z. Luo & S.T. Wu (2015). OLED Versus LCD: Who Wins? Optics and Photonics News, 19-21.
[4] J. Han & H. J. Suk. (2019). Do users perceive the same image differently? Comparison of OLED and LCD in mobile HMDs and smartphones. Journal of Information Display, 20(1), 31–38. https://doi.org/10.1080/15980316.2019.1567612
[5] X. Liang, J. Xia, G. Dong, B. Tian, & L. M. Peng. (2016). Carbon Nanotube Thin Film Transistors for Flat Panel Display Application. In Topics in Current Chemistry (Vol. 374, Issue 6). Springer Verlag. https://doi.org/10.1007/s41061-016-0083-6
[6] M. E. Miller. (2019). LCD Display Technology (pp. 87–105). https://doi.org/10.1007/978-3-030-02834-3_5
[7] F. W. John. (2020). TFT Technology: Advancements and Opportunities for Improvement. Frontline Technology, 9-13.
[8] M. Tulej, N. F. W. Ligterink, C. de Koning, V. Grimaudo, R. Lukmanov, P.K. Schmidt, A. Riedo, & P. Wurz. (2021). Current progress in femtosecond laser ablation/ionisation time-of-flight mass spectrometry. In Applied Sciences (Switzerland) (Vol. 11, Issue 6). MDPI AG. https://doi.org/10.3390/app11062562
[9] B. Kumar, B. K. Kaushik, & Y. S. Negi. (2014). Organic thin film transistors: Structures, models, materials, fabrication, and applications: A review. Polymer Reviews, 54(1), 33–111. https://doi.org/10.1080/15583724.2013.848455
[10] M. G. Faraj, K. Ibrahim. (2011). PET as a plastic substrate for the flexible optoelectronic applications Fabrication of flexible thin films by spray pyrolisis technique. In Optoelectronics and Advanced Materials-Rapid Communications (Vol. 5, Issue 8), 879-882. https://www.researchgate.net/publication/224880095
[11] J. Prakash, J. C. Pivin & H. C. Swart. (2015). Noble metal nanoparticles embedding into polymeric materials: From fundamentals to applications. In Advances in Colloid and Interface Science (Vol. 226, pp. 187–202). https://doi.org/10.1016/j.cis.2015.10.010
[12] T. Nishi, T. Mayama, H. Ohta, & Y. Okamoto. (2019). Annealing cycle dependence of thermal conductivity for Si-Ge-Au thin film analyzed by thermal microscopy. Sensors and Materials, 31(3), 743–749. https://doi.org/10.18494/SAM.2019.2119
[13] M. Shindo, T. Sawada, K. Doi, K. Mukai & K. Shudo. (2013). Spectroscopic analysis of a nanostructure roughness of plasma-deposited Au films using organic monolayer. Journal of Physics: Conference Series, 441(1). https://doi.org/10.1088/1742-6596/441/1/012044
[14] T. S. Dorofeeva & E. Seker. (2016). In situ electrical modulation and monitoring of nanoporous gold morphology. Nanoscale, 8(47), 19551–19556. https://doi.org/10.1039/c6nr07237b
[15] A. Petzold, J. Strom, S. Ohlsson, & F. P. Schroder. (1998). Elemental composition and morphology of ice-crystal residual particles in cirrus clouds and contrails. In Atmospheric Research, Vol. 49, 21-34.
[16] A. Hacini, A. H. Ali, & N. N. Adnan. (2021). Optimization of ITO thin film properties as a function of deposition time using the Swanepoel method. Optical Materials, 120, 1-10. https://doi.org/10.1016/j.optmat.2021.111411
[17] H. Howari. (2019). Pulsed Laser Annealing Effect on Optical and Structural Properties of ZnS/ZnSe Heterostructures. Journal of Modern Materials, 6(1), 23–29. https://doi.org/10.21467/jmm.6.1.23-29

[18] K. Isiyaku, A. H. Ali, A., & N. Nayan. (2020). Characterisation of Laser-Treated Ag, Al, and Al/Ag Metal Thin Films Deposited by DC Sputtering. In International Journal of Nanoelectronics and Materials (Vol. 13, Issue 1).
[19] Yunus, Z. M., & Azaha, N. A. N. (2021). Jackfruit Seeds Starch-Based Coagulant for Synthetic Textile Wastewater Remediation. *Enhanced Knowledge in Sciences and Technology*, *1*(2), 72-80.
[20] SATRIA, A. H. B. M. (2022). Isolation and characterization of biosurfactant-producing lactic acid bacteria from sauerkraut. *Enhanced Knowledge in Sciences and Technology*, *2*(2), 060-069.